

RESEARCH ARTICLE

A competence-regulated toxin-antitoxin system in *Haemophilus influenzae*Hailey Findlay Black^{1#a}, Scott Mastromatteo^{1#b}, Sunita Sinha², Rachel L. Ehrlich³, Corey Nislow⁴, Joshua Chang Mell³, Rosemary J. Redfield^{1*}**1** Department of Zoology, University of British Columbia, Vancouver, British Columbia, Canada,**2** Sequencing + Bioinformatics Consortium, Office of the Vice-President, University of British Columbia, Vancouver, British Columbia, Canada, **3** Department of Microbiology & Immunology, Center for Genomic Sciences, Drexel University College of Medicine, Philadelphia, Pennsylvania, United States of America,**4** Department of Pharmaceutical Sciences, University of British Columbia, Vancouver, British Columbia, Canada

#a Current address: Dept. of Medical Genetics, University of British Columbia, Vancouver, British Columbia Canada

#b Current address: Program in Genetics and Genome Biology, The Hospital for Sick Children, Toronto, Ontario, Canada

* redfield@zoology.ubc.ca

OPEN ACCESS

Citation: Findlay Black H, Mastromatteo S, Sinha S, Ehrlich RL, Nislow C, Chang Mell J, et al. (2020) A competence-regulated toxin-antitoxin system in *Haemophilus influenzae*. PLoS ONE 15(1): e0217255. <https://doi.org/10.1371/journal.pone.0217255>

Editor: Günther Koraimann, University of Graz, AUSTRIA

Received: May 3, 2019

Accepted: December 16, 2019

Published: January 13, 2020

Copyright: © 2020 Findlay Black et al. This is an open access article distributed under the terms of the [Creative Commons Attribution License](https://creativecommons.org/licenses/by/4.0/), which permits unrestricted use, distribution, and reproduction in any medium, provided the original author and source are credited.

Data Availability Statement: RNA-seq data were deposited with NCBI under BioProject 293882.

Funding: This work was supported by funding from Canadian Institutes of Health Research to R.J.R., an NIH F32 AI084427 grant to J.C.M., and NIH R01 DC002148 to Garth D. Ehrlich. The funders had no role in study design, data collection and analysis, decision to publish, or preparation of the manuscript.

Competing interests: The authors have declared that no competing interests exist.

Abstract

Natural competence allows bacteria to respond to environmental and nutritional cues by taking up free DNA from their surroundings, thus gaining both nutrients and genetic information. In the Gram-negative bacterium *Haemophilus influenzae*, the genes needed for DNA uptake are induced by the CRP and Sxy transcription factors in response to lack of preferred carbon sources and nucleotide precursors. Here we show that one of these genes, *H10659*, encodes the antitoxin of a competence-regulated toxin-antitoxin operon (*toxTA*), likely acquired by horizontal gene transfer from a *Streptococcus* species. Deletion of the putative toxin (*H10660*) restores uptake to the antitoxin mutant. The full *toxTA* operon was present in only 17 of the 181 strains we examined; complete deletion was seen in 22 strains and deletions removing parts of the toxin gene in 142 others. In addition to the expected Sxy- and CRP-dependent-competence promoter, *H10659/660* transcript analysis using RNA-seq identified an internal antitoxin-repressed promoter whose transcription starts within *toxT* and will yield nonfunctional protein. We propose that the most likely effect of unopposed toxin expression is non-specific cleavage of mRNAs and arrest or death of competent cells in the culture. Although the high frequency of *toxT* and *toxTA* deletions suggests that this competence-regulated toxin-antitoxin system may be mildly deleterious, it could also facilitate downregulation of protein synthesis and recycling of nucleotides under starvation conditions. Although our analyses were focused on the effects of *toxTA*, the RNA-seq dataset will be a useful resource for further investigations into competence regulation.

Introduction

Bacterial toxin-antitoxin gene pairs were originally discovered on plasmids, where they function to promote plasmid persistence by killing any daughter cells that have not inherited the plasmid. Typically, one gene of the pair encodes a relatively stable toxic protein that blocks cell growth, and the other encodes a labile antitoxin (RNA or protein) that blocks the toxin's activity and limits its transcription [1,2]. Toxin-antitoxin gene pairs have also been discovered on many bacterial chromosomes, where they are thought to be relatively recent introductions that in some cases have been co-opted to regulate cellular functions or provide other benefits [3]. Here we describe one such system, which is induced in naturally competent cells and whose unopposed toxin completely prevents DNA uptake and transformation.

Many bacteria can become naturally competent, able to take up DNA from their surroundings and—when sequence similarity allows—recombine it into their genomes [4,5,6]. In most species, DNA uptake is tightly controlled, with protein machinery specified by a set of co-regulated chromosomal genes induced in response to diverse cellular signals. Genes in the competence regulon encode not only components of the DNA uptake machinery that moves DNA across the outer membrane of the cell, but proteins that translocate DNA across the inner membrane, proteins that facilitate recombination, and proteins of unknown function. *Haemophilus influenzae* has an unusually small and well-defined competence regulon (26 genes in 13 operons) induced by signals of energy and nucleotide scarcity [7,8]. Induction of these genes begins in response to depletion of phosphotransferase sugars. The resulting rise in cyclic AMP (cAMP) activates the transcription factor CRP, and the CRP/cAMP complex then stimulates transcription of genes with canonical CRP-promoter elements (CRP-N genes). Most of these genes help the cell to use alternative carbon sources, but one encodes the competence-specific transcriptional activator Sxy. However, efficient translation of *sxy* mRNA occurs only when purine pools are also depleted [9,10]. If both signals are active, Sxy then acts with CRP at the promoters of competence genes, stimulating their transcription and leading to DNA uptake and natural transformation. These competence promoters are distinguished by the presence of 'CRP-S' sites (formerly called CRE sites), variants of standard CRP sites that depend on both CRP and Sxy for activation [11]. Development of competence thus requires the CRP/cAMP complex twice, first for *sxy* transcription (at its CRP-N promoter) and then for transcription of the competence genes (at their CRP-S promoters). As is common in competence systems, only some of the cells in the population become competent (typically 10–50%).

Of the fifteen Sxy-regulated *H. influenzae* genes needed for DNA uptake, all but one encode typical competence proteins—membrane-associated proteins homologous to known components of the Type IV pilus-based DNA uptake machinery present in nearly all known naturally competent species [5]. The one exception is *HI0659*, which instead encodes a predicted 98 amino acid cytoplasmic protein with no similarity to known DNA uptake proteins. It shares a competence-inducible CRP-S promoter with an upstream gene encoding another short cytoplasmic protein (*HI0660*, 119 aa) (Fig 1, top). Although a knockout of *HI0659* eliminates detectable DNA uptake and transformation, a knockout of *HI0660* has no effect [8].

Here we show that *HI0660* and *HI0659* comprise a horizontally transferred operon that encodes a toxin-antitoxin pair, and that expression of the toxin in the absence of the antitoxin completely prevents DNA uptake and transformation. Surprisingly, expression of this toxin has only modest effects on induction of competence genes and on cell growth and viability.

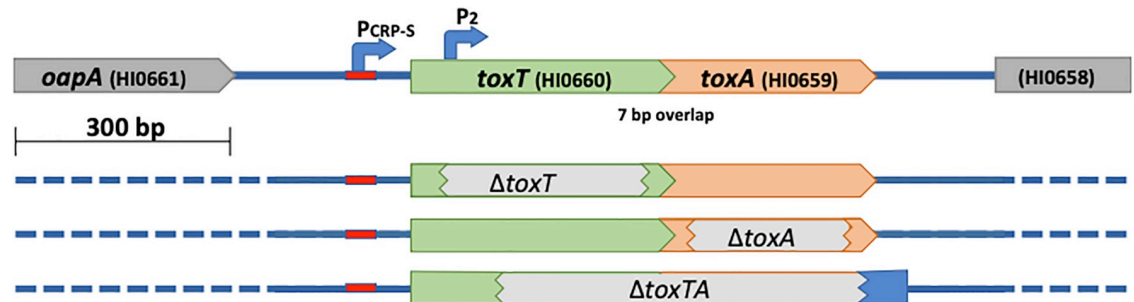


Fig 1. Structure of wildtype and mutant *toxTA* genes. Top line: structure of the wildtype *toxTA* operon in strain Rd KW20. Lower lines: grey bars indicate segments deleted in $\Delta toxT$, $\Delta toxA$, and $\Delta toxTA$ mutants.

<https://doi.org/10.1371/journal.pone.0217255.g001>

Results

HI0659 and HI0660 show homology to type II toxin/antitoxin systems

Our original analyses of competence-induced genes did not identify any close homologs of *HI0659* or *HI0660* [7,8]. However subsequent database searches and examination of BLAST results revealed that these genes' products are homologous to genes annotated as belonging to Type II toxin/antitoxin families, which consists of a two-gene operon encoding the toxin and antitoxin components [2]. *HI0660* is annotated on NCBI as a phage-related protein containing the COG4679 region found in members of the ParE toxin family. The Pfam and TAFinder databases assign the *H. influenzae* *HI0660* protein to the ParE/RelE toxin superfamily, whose characterized members include both gyrase inhibitors and ribonucleases that arrest cell growth by cleaving mRNAs and other RNAs [2,12,13]. The *HI0659* protein is annotated in NCBI as containing a helix-turn-helix-XRE DNA-binding domain, which is commonly found in promoter-binding antitoxins [14]. Structurally, the Phyre2 modelling software predicts that the best match of known structure for *HI0660* is the HigB toxin of *Streptococcus pneumoniae* (100% confidence across 95% of the protein sequence), and the best match for *HI0659* is the HigA antitoxin of *Streptococcus pneumoniae* (99.9% confidence across 92% of the protein sequence) [15].

HI0659 and HI0660 act as a toxin-antitoxin system that affects natural competence

If *HI0660* and *HI0659* do encode a toxin-antitoxin pair as suggested by *in silico* analyses, then $\Delta HI0659$'s DNA uptake defect would likely be caused by unopposed expression of a *HI0660*-encoded toxin protein that prevents DNA uptake, and knocking out this toxin gene would restore competence to the *HI0659* (antitoxin⁻) mutant. We tested this by constructing an *HI0660/HI0659* double mutant (Fig 1) and examining its ability to be transformed with antibiotic-resistant chromosomal DNA (MAP7) compared to wild type or either single mutant. The double mutant had normal transformation (Fig 2, black bars), showing that mutation of *HI0660* suppresses the competence defect of an *HI0659* mutant, and also that neither *HI0660* nor *HI0659* is directly needed for the development of competence. This supported the postulated antitoxin function of *HI0660*, so we named the *HI0660* and *HI0659* genes *toxT* (toxin) and *toxA* (antitoxin) respectively.

Phylogenetic evidence for lateral transfer of *toxTA*

Since toxin/antitoxin operons are often highly mobile [14], we examined the distribution of *toxTA* homologs in other strains and species (Fig 3). These homology searches were performed

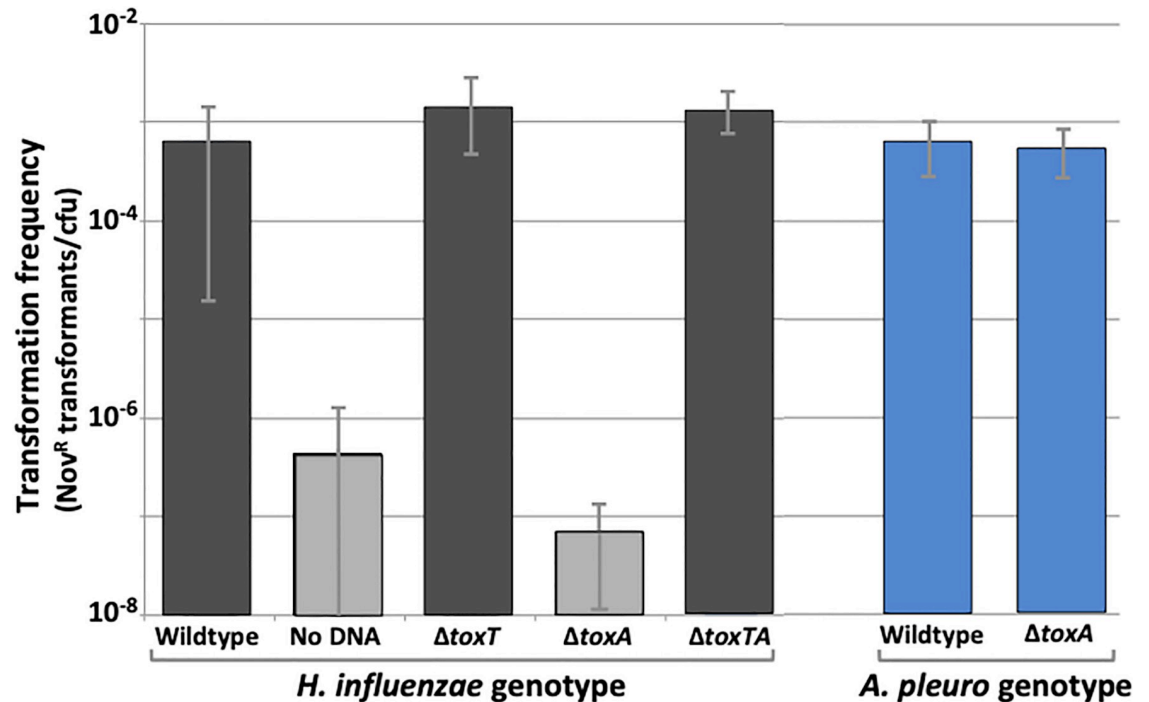


Fig 2. Transformation phenotypes of wildtype cells and *toxTA* mutants. Competence-induced cultures were incubated with MAP7 chromosomal DNA, and transformation frequencies were calculated as the novobiocin resistant (Nov^R) colonies per colony forming unit (CFU). Bars represent the means of at least three biological replicates, with error bars representing one standard deviation. Grey bars indicate values below the detection limit ($\sim 10^{-8}$ CFU/ml).

<https://doi.org/10.1371/journal.pone.0217255.g002>

using NCBI's tBLASTn function to search for homologs of a protein by querying translated nucleotide sequence databases; this function was used because toxin and antitoxin proteins are often missed in protein annotations due to their small size. Complete or partial *toxTA* operons were found at the same genomic location in most *H. influenzae* genomes and in the closely related *H. haemolyticus* (see below), but there were no recognizable homologs in most other bacteria, including most other members of the Pasteurellaceae. Instead, most identifiable homologs (with about 60% amino acid identity) were in a very distant group, the Firmicutes, mainly within the streptococci. Ninety-six of the top 100 tBLASTn hits to *ToxT* outside the Pasteurellaceae were to diverse *Streptococcus* species. This suggests that the *toxTA* operon may have been transferred from a Firmicute into a recent ancestor of *H. influenzae* and *H. haemolyticus*. When we excluded *Streptococcus* from the BLAST search, sporadic matches were found in a wide variety of other taxa. In addition, *toxTA* operons with about 50% identity were found in one other small distant Pasteurellacean subclade (*Actinobacillus sensu stricto*), and on two 11kb plasmids (pRGRH1858 and pRGFK1025) from an uncultured member of a rat gut microbiome and an uncultivated *Selenomonas* sp. The genes flanking the *A. pleuropneumoniae* homologs are unrelated to those flanking HI0659 and HI0660, and an *A. pleuropneumoniae* *toxA* knockout mutant had normal growth and competence (Figure A in S1 File). The distribution of *toxTA* homologs across taxa is summarized in Fig 3A.

To examine the potential for of gene transfer events in the two Pasteurellaceae sub-clades, we created an unrooted maximum likelihood phylogeny from the concatenated alignment of *toxT* and *toxA* amino acid sequences from selected species where both genes were found (Fig 3B). There was 99% bootstrap support for a node which branches into the *Haemophilus*, *Actinobacillus*, and *Streptococcus* clades (which also group with the plasmid samples). In isolation,

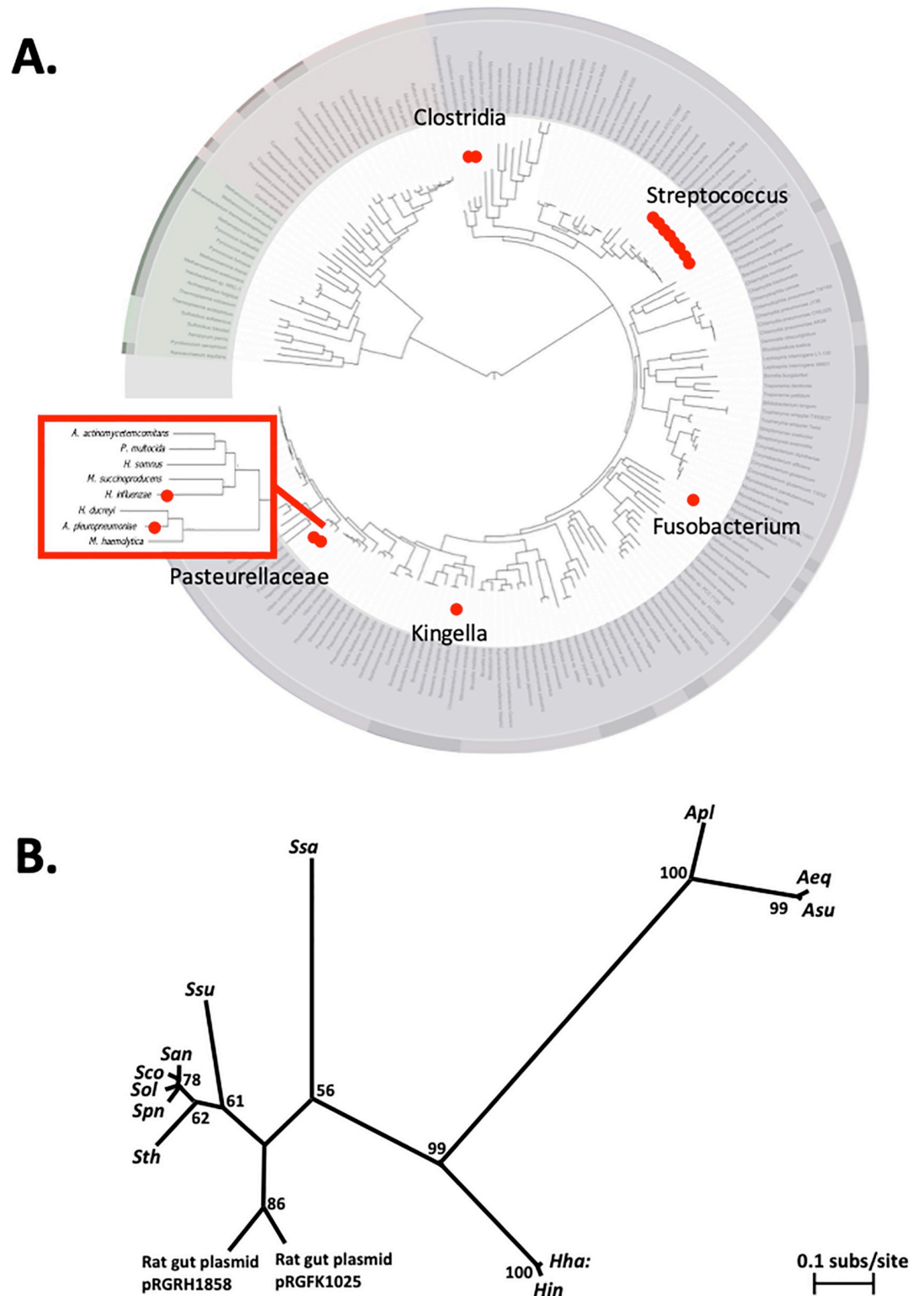


Fig 3. Distribution of *toxTA* homologs in bacterial genomes. A. Summary of tBLASTn results. Red dots indicate one or more taxa containing homologs of both ToxT and ToxA. Bacterial phylogeny image from Wikimedia Commons [16]. Inset: Pasteurellacean phylogeny from Redfield *et al.* 2006. B. Unrooted maximum likelihood phylogeny of concatenated ToxT and ToxA homologs from selected species where both were detected. Numbers at nodes are bootstrap values. Species abbreviations: *Apl*: *Actinobacillus pleuropneumoniae*; *Aeq*: *A. equuli*; *Asu*: *A. suis*; *Haemophilus haemolyticus*; *Hin*: *H.*

influenzae; *Ssa*: *Streptococcus salivarius*; *Ssu*: *S. suis*; *San*: *S. anginosus*; *Sco*: *S. constellatus*; *Sol*: *S. oligofermentans*; *Spn*: *S. pneumoniae*; *Sth*: *S. thermophilus*.

<https://doi.org/10.1371/journal.pone.0217255.g003>

this branching pattern could be consistent with a single Pasteurellacean origin of the toxin-antitoxin pair, but the absence of homologs from all other Pasteurellaceae makes a single Pasteurellacean origin unlikely, since it would require multiple deletions in other Pasteurellacean subclades or a near-simultaneous within-clade lateral transfer. Since the *Actinobacillus* sequences showed higher identity to *Streptococcus* sequences than to the *Haemophilus* sequences, the two Pasteurellacean groups are more likely to have acquired their *toxTA* operons by independent lateral transfers, perhaps from Firmicutes. However, because we were unable to root our tree, we cannot unequivocally determine the presence or direction of any gene transfer events. We were unable to use synteny to determine whether the gene pair was gained in the same insertion event because in *Actinobacillus* species, the upstream and downstream genes flanking *ToxTA* in *Haemophilus influenzae* are not adjacent to one another nor to the *Actinobacillus* *ToxTA* homologs. Examination of flanking genes within the *Streptococci* was broadly consistent with inheritance of the *ToxTA* homologs from a common ancestor, but was not possible in all cases due to genomic rearrangements which separated the flanking genes.

Deletions in *H. influenzae* *toxT* are common

The presence of an intact and syntenic *toxTA* operon in *H. haemolyticus* shows that the presence of *toxTA* is the ancestral *H. influenzae* state. Of the 181 *H. influenzae* genome sequences available in public databases (described in Table B of S1 File), 162 had recognizable *toxA* sequences. All of these encoded full length ToxA proteins, but all except 24 had one of two common deletions affecting *toxT*. The extents of these deletions are shown by the grey bars at the bottom of Fig 4. The most common deletion ($n = 97$) removed 178 bp of *toxT* coding sequence but left both promoters intact. The second ($n = 45$) removed 306 bp of sequence including both *toxTA* promoters and the *toxT* start codon. The 19 genomes that lacked recognizable *toxA* sequences all had the same 1015 bp deletion removing both *toxT* and *toxA* but leaving the flanking genes intact. In place of the missing sequences were 87 bp with no high-scoring BLAST alignments in GenBank. This collection of strains is from diverse times, locations and body sites, and the deletion distribution suggests that deletions inactivating *toxT* arise rarely but are favoured by selection. The average pairwise distance among the 162 *toxA*

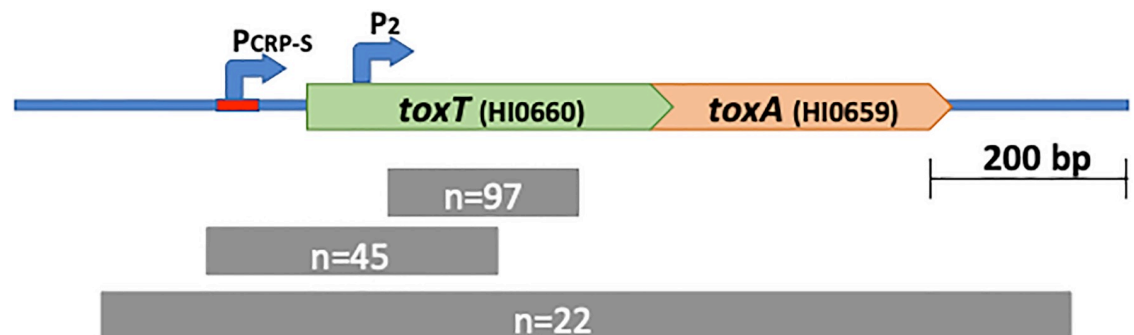


Fig 4. Natural deletions in the *toxTA* operon. Top line: structure of the wildtype *toxTA* operon in strain KW20. Lower lines: grey bars indicate the spans of the three naturally occurring deletions among the 181 available sequences, annotated with the number of sequences with each deletion.

<https://doi.org/10.1371/journal.pone.0217255.g004>

genes is 0.106, slightly higher than the average of all genes with one copy per strain (0.088). The d_N/d_S ratio of 0.037 is lower than that of the average gene (0.243), indicating mild purifying selection on *toxA*. However, this may underestimate the strength of selection, since most *toxAs* lack functional *toxT*, no strains with *toxT* only were seen, and the operon may not be expressed due to upstream deletions. Both sequence divergence and the high frequency of *toxT* deletions agree with expectations for a toxin/antitoxin system whose antitoxin protects against a toxin that is at least mildly deleterious.

Variation in *toxTA* does not correlate with strain-specific variations in DNA uptake and transformation

Maughan and Redfield [17] measured the ability of 34 *H. influenzae* strains to both take up DNA and become transformed, so we examined this data for correlations with the presence of *toxTA* in the 19 of these strains whose *toxTA* genotypes we were able to determine from genome assemblies (Table C of S1 File). All but one of the 19 strains had a complete *toxA* coding sequence but only five had intact *toxTA* operons. Of the rest, four had the large deletion that removed both *toxTA* promoters, nine had the smaller deletion internal to *toxT*, and one had the 1015 bp complete deletion. No obvious correlation was seen between the *toxTA* genotypes and the DNA uptake, transformation or growth phenotypes, but there was insufficient data for a high-powered analysis using allelic variation.

Growth and competence phenotypes of *H. influenzae toxTA* mutants

Earlier investigation of DNA uptake and transformation by the *H. influenzae toxA* knockout strain found that both were below the limit of detection (>100 -fold reduction and $>10^6$ -fold reduction respectively) after the standard competence-inducing treatment [8] (see also Fig 2), although there was no apparent growth defect in rich medium. Figure B in S1 File confirms the non-transformability of $\Delta toxA$ cells both in log phase growth and at intermediate time points during competence induction.

A simple explanation for this defect would be that unopposed ToxT prevents competence, when not opposed by ToxA, by killing or otherwise inactivating the (competence-induced) cells in which it is expressed. To detect effects of unopposed expression of *toxT* toxin, we analyzed growth rates of wildtype and $\Delta toxA$ strains (Fig 5) before, during, and after transfer to the competence-inducing starvation medium MIV. The first 60 min of Fig 5 show that unopposed expression of *toxT* toxin slightly slows exponential growth in rich medium. A more detailed analysis of growth of rich-medium cultures wells is provided in Figure C in S1 File, using 20 replicate wells of a BioScreen culture plate for each strain (see Methods for details); the growth defect of the $\Delta toxA$ strain is barely detectable under this condition. This lack of a severe growth defect is not surprising; because the *toxTA* promoter is regulated by a CRP-S site, its expression (and thus ToxT production) might be limited to competent cells even in the absence of ToxA [7]. The grey-shaded portion of Fig 5 shows cell growth after transfer to MIV (samples between 70 min and 165 min). Cells transferred to MIV usually undergo only one or two doublings, and deletion of *toxA* delays this but does not eliminate it (see also Figure D in S1 File). Cells returned to rich medium from MIV might be delayed in their recovery, if unopposed toxin expression during competence development kills cells or halts growth. However, both strains had similar recovery kinetics after a fraction of their culture was returned to rich medium, although $\Delta toxA$ cells again grew slightly slower than wildtype (175–230 min in Fig 5). Figure E in S1 File shows the OD₆₀₀ readings corresponding to the CFU/ml data shown in Fig 5. These agree well, showing that differences in cell growth can be explained by the differences in cell division.

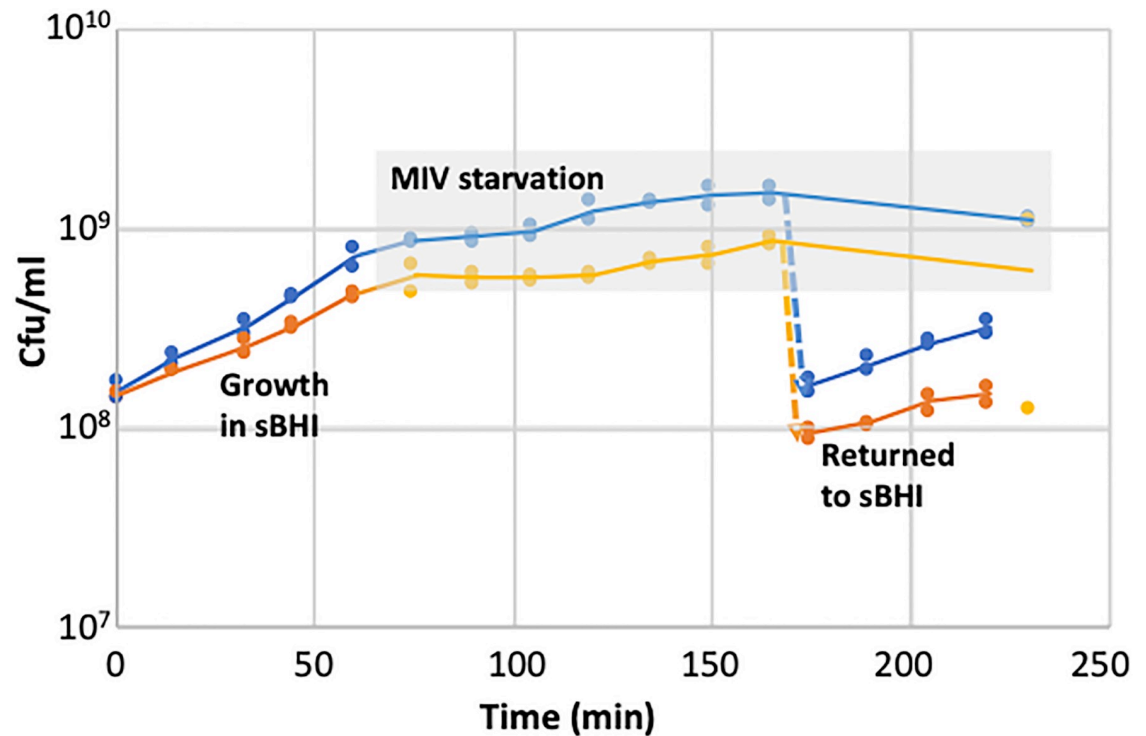


Fig 5. Growth of *H. influenzae* wildtype and $\Delta toxA$ cells before, during and after competence induction. Two independent cultures of log-phase cells in sBHI were transferred to MIV at $t = 65$ min; a portion of each MIV culture was diluted 10-fold into sBHI at $t = 170$ min. The grey-shaded area indicates samples taken from MIV cultures. Blue: KW20, orange: $\Delta toxA$. Figure E in [S1 File](#) shows the corresponding OD600 values.

<https://doi.org/10.1371/journal.pone.0217255.g005>

Since cyclic AMP is required for normal induction of the competence genes, and addition of cAMP induces partial competence during exponential growth [18], we also tested the effect of cAMP on the $\Delta toxA$ knockout. Addition of cAMP did not rescue its transformation defect (Figure F in [S1 File](#)), so failure to transform is not caused by defective cAMP production in the antitoxin mutant.

Since some chromosomal toxin-antitoxin systems have acquired beneficial roles in modulating cell growth [19], we also examined whether the absence of toxin changed growth and competence under various conditions. The grey line in Figure C in [S1 File](#) shows that, under BioScreen growth assay conditions, $\Delta toxT$'s growth was indistinguishable from that of wild-type cells (blue line), and [Fig 2](#) shows that its MIV-induced competence is also unchanged. Figure G in [S1 File](#) shows that the kinetics of $\Delta toxT$ competence development and loss during growth in rich medium were also indistinguishable from wildtype. We conclude that ToxT's normal expression in cells expressing antitoxin does not detectably regulate growth or the development or loss of competence. Unfortunately, inferring the relationship between competence and growth is complicated because many cells in 'competent' cultures are unable to transform. In some species the non-transformable cells are known to have not induced their competence genes, but this has not been investigated for *H. influenzae*.

Transcriptional control of competence

Since these phenotypic analyses gave little evidence of MIV-specific toxicity or insight into the cause of the competence defect, we used RNA-seq to investigate how *toxTA* is regulated and how mutations affect transcript levels of competence genes. In these experiments, samples for

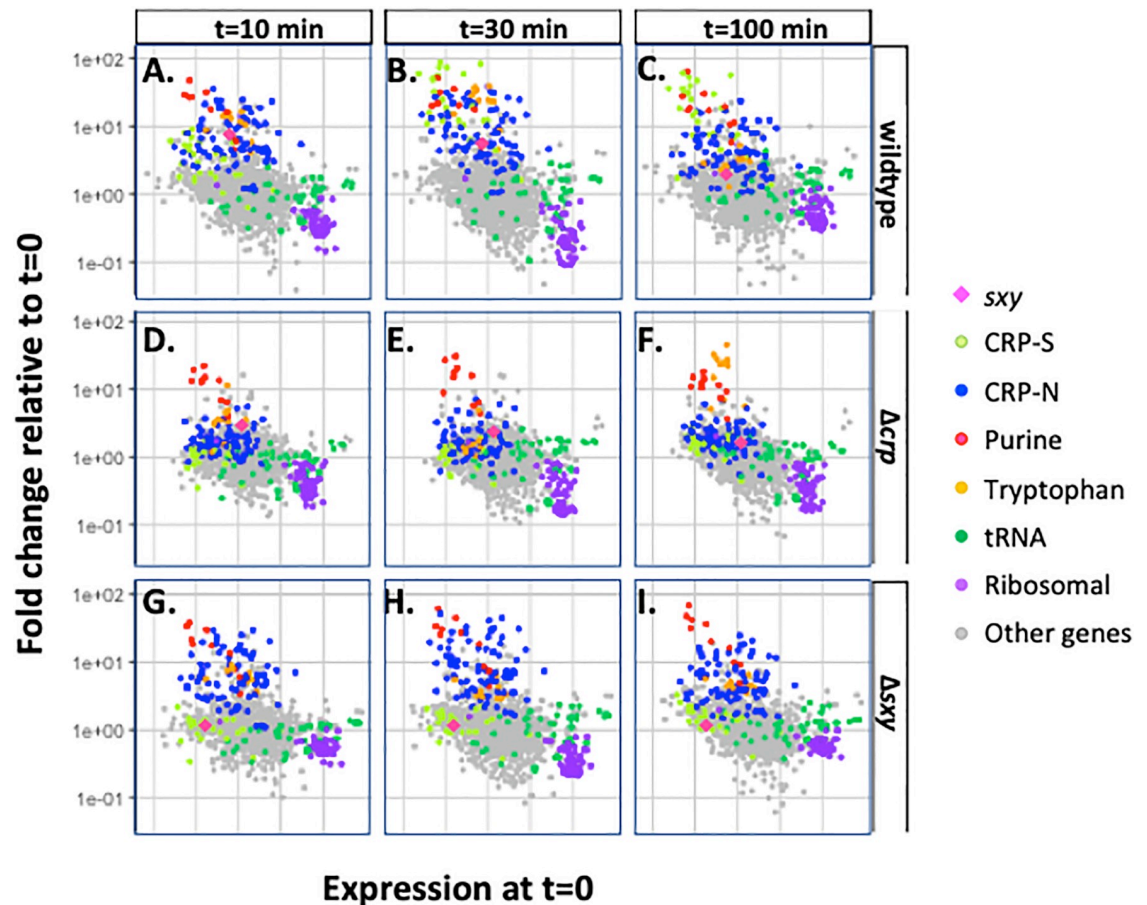


Fig 6. Competence-induced changes in transcript levels of *H. influenzae* genes regulated by CRP and Sxy. Each dot represents a gene, colour-coded by function: pink diamond: *sxy*; light green dot: CRP-S-regulated; blue dot: CRP-N-regulated; red dot: purR regulon; yellow dot: tryptophan regulon; dark green dot: tRNA; purple dot: ribosomal proteins; grey dot: other or unknown functions. Each dot's horizontal position indicates the gene's relative transcript level (as FPKM) in rich medium ($t = 0$) and its vertical position indicates how this level changed at later time points (A: $t = 10$; B: $t = 30$; C: $t = 100$) or in a mutant background at $T = 30$ (D-F; Δcrp ; G-I: Δsxy).

<https://doi.org/10.1371/journal.pone.0217255.g006>

RNA preparations were taken from three replicate cultures at four time points, first when cells were growing in log phase in the rich medium sBHI ($t = 0$), and then at 10, 30 and 100 minutes after each culture had been transferred to MIV. We first examined how competence induction in wildtype and regulatory-mutant cells changed transcript levels of genes known to be regulated by CRP and CRP+Sxy (CRP-N and CRP-S genes respectively). Fig 6 gives an overview of the results. The top row shows competence-induced changes in transcript abundances in wildtype cells at 10, 30 and 100 minutes, and the lower rows show that some of these changes do not occur in Δcrp and Δsxy cells. Each coloured dot represents a gene, colour-coded by function. Its horizontal position indicates its transcript level in rich medium ($T = 0$) and its vertical position indicates how this level changed in MIV (top row—wildtype cells, lower rows, Δcrp and Δsxy cells). Thus in Fig 6A the higher positions of the dark blue dots (genes regulated by CRP-N sites) and the red diamond (the competence regulator *sxy*) indicate that they were strongly induced after 10 min in MIV. Induction of *sxy* was followed at 30 and 100 minutes by strong induction of the known competence-regulon genes (higher positions of CRP-S genes; light green dots) (Fig 6B and 6C). Note that transcript levels are relative; because of population

heterogeneity they may underestimate the degree of induction or downregulation in the cells that go on to become competent. Consistent with prior studies [7], induction of all these genes was blocked by deletion of the *crp* gene (Fig 6D–6F), and induction of the competence regulon (CRP-S) genes was blocked by deletion of *sxy* (Fig 6G–6I). Analysis of other competence-associated changes in transcript levels in normal cells and in Δcrp and Δsxy mutants is provided in the Supplementary Materials.

Transcriptional control of *toxTA*

RNA-seq analysis confirmed that *toxTA* is regulated as a typical competence operon. In wild-type cells, baseline RNA-seq levels of *toxT* and *toxA* transcripts were very low during log phase in rich medium, with approximately tenfold induction after 30 minutes incubation in MIV (green lines and points in Fig 7 (*toxT*) and Figure H in S1 File (*toxA*). As expected, this increase was eliminated by knockouts of CRP and Sxy (brown and blue lines and points in Fig 7 and Figure H in S1 File). Like other CRP-S genes, both *toxT* and *toxA* were also strongly induced in rich medium by *sxy* and *murE* mutations known to cause hypercompetence [20,21] and by a newly identified hypercompetence mutation in *rpoD* (Figure I in S1 File). Thus the *toxTA* operon is regulated as a typical member of the competence regulon.

RNA-seq analysis also showed that the *toxTA* operon is regulated as a typical type II toxin-antitoxin operon. In such operons, the antitoxin protein usually binds to the toxin protein, which protects cells from the toxin in two ways. First, antitoxin binding inactivates the toxin. Second, it also activates the antitoxin component as a repressor of the *toxTA* promoter [2,22]. *H. influenzae* ToxA has a HTH-XRE DNA-binding domain, which is commonly found in promoter-binding antitoxins [1,14], and the RNA-seq analysis in Fig 7 strongly suggests that it represses *toxTA* transcription. The $\Delta toxA$ mutant retains an intact *toxTA* promoter and *toxT* coding sequence (see Fig 1); it had 9-fold increased baseline transcript levels of *toxT* in log phase cells (red line and points in Fig 7). Transcript levels increased further during

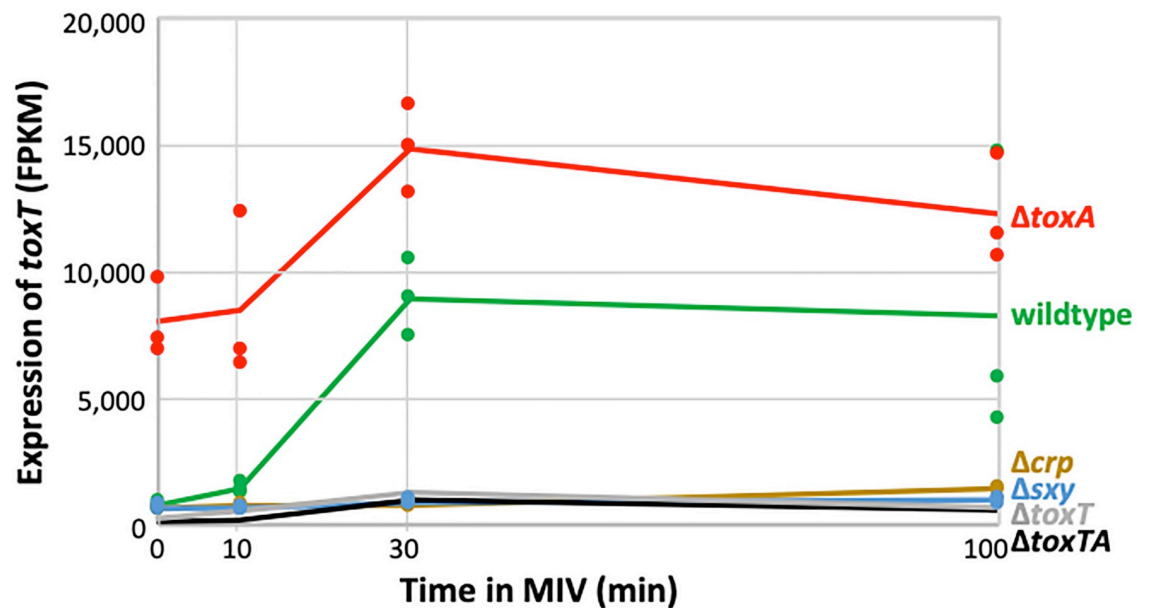


Fig 7. Competence-induced changes in transcript level of *H. influenzae* *toxT*. Sample FPKM values (dots) and means (lines) for *toxT* (HI0660). Strains: wildtype: green; Δcrp : brown; Δsxy : blue; $\Delta toxA$: red; $\Delta toxT$: grey; $\Delta toxTA$: black. The values for the $\Delta toxT$ and $\Delta toxTA$ samples are underestimates because most of the gene has been deleted in these strains.

<https://doi.org/10.1371/journal.pone.0217255.g007>

competence development, with the same kinetics as in wildtype cells, suggesting independent contributions from baseline repression by antitoxin and competence induction by CRP and Sxy. (Values for *toxT* transcript levels are shown by the red points and line in Figure H in [S1 File](#), but are underestimates because most of the gene has been deleted).

Because most antitoxins have only weak affinity for DNA in the absence of their cognate toxin, ToxA was predicted to repress *toxTA* only when bound to ToxT. Therefore, we were initially surprised that knocking out *toxT* or both *toxT* and *toxA* did not increase RNA-seq coverage of residual *toxT* sequences ([Fig 7](#), grey and black lines) and that knocking out both genes did not increase coverage of residual *toxA* (grey line in Figure H in [S1 File](#)). These deletion mutants retain all the *toxTA* upstream sequences and the *toxT* start codon, and enough sequence of the deleted genes to identify them in the RNA-seq analysis. An explanation was suggested by a recent study of the *Escherichia coli* *hicAB* toxin/antitoxin system [23], and confirmed by more detailed analysis of *toxTA* transcripts. The HicA (toxin) and HicB (antitoxin) proteins have no detectable sequence homology to ToxT and ToxA, but their operon is similarly regulated by Sxy and has the same atypical organization (toxin before antitoxin) [24]. Turnbull and Gerdes [23] showed that the *hicAB* operon has two promoters. Promoter P1 has a CRP-S site regulated by CRP and Sxy, which is not repressed by the HicB antitoxin. A secondary promoter P2 is very close to the *hicA* start codon; it is repressed by HicB independently of HicA, and its shortened transcripts produce only functional HicB, not HicA. Promoter P1 of this *hicAB* system thus resembles the CRP-S regulation of the *toxTA* operon, and the presence of a second antitoxin-regulated internal promoter similar to P2 would explain the high *toxTA* operon transcript level seen in the *toxA* knockouts. This finding prompted us to do a more detailed analysis of *toxTA* transcription patterns in wildtype and mutant cells to determine whether the *toxTA* transcripts expressed in the absence of *toxA* were similarly truncated. [Fig 8A](#) shows RNA-seq coverage of the *toxTA* promoter region and the 5' half of *toxT*, in wildtype cells (green) and in the *toxA* deletion mutant (purple). As expected, the predicted CRP-S promoter upstream of *toxTA* was only slightly active at T = 10 but strongly induced at T = 30 and T = 100 (note log scale); its activity was not affected by deletion of *toxA*. Deletion of *toxA* instead caused strong constitutive transcription from a second promoter ('P2'), with reads beginning about 30 bp downstream of the *toxT* start codon. Transcripts with this 5' end are unlikely to produce active ToxT; the only other in-frame AUG in *toxT* is 30 bp from the end of the gene, and it and the first GUG (position 35) lack Shine-Dalgarno sequences. This supports the hypothesis that the *H. influenzae* *toxTA* operon is regulated similarly to the *E. coli* *hicAB* operon, with Sxy-induced transcription from a CRP-S promoter and antitoxin-repressed transcription from a downstream 'P2' promoter whose transcript produces antitoxin but not toxin.

In the *E. coli* *hicAB* system, P2 is repressed by HicB antitoxin alone, binding of HicB to the P2 operator is destabilized when HicA toxin is abundant, and transcription from P2 in plasmid constructs is elevated when the chromosomal *hicAB* operon is deleted [23]. To look for parallels in *H. influenzae*'s *toxTA*, we more precisely measured transcription in wildtype and *toxTA* mutant cells by scoring the coverage at two positions in the *toxTA* operon; each is indicated by a red vertical line at the bottom of [Fig 8A](#). Position 0 is the *toxT* start codon, 34 nt downstream from the CRP-S promoter (P_{CRP-S}) but upstream of the putative P2 promoter, and position 100 is 70 nt downstream from P2 (P2 and position 100 are deleted in $\Delta toxT$). To eliminate read-mapping artefacts arising from failure of reads that span an insertion or deletion to align to the reference sequence, each mutant's reads were instead mapped onto its own *toxTA* sequence. Comparison of [Fig 8B and 8C](#) shows that coverage at position 100 was always higher than coverage at position 0, consistent with the presence of a second promoter between positions 0 and 100. [Fig 8B](#) also shows that coverage at position 0

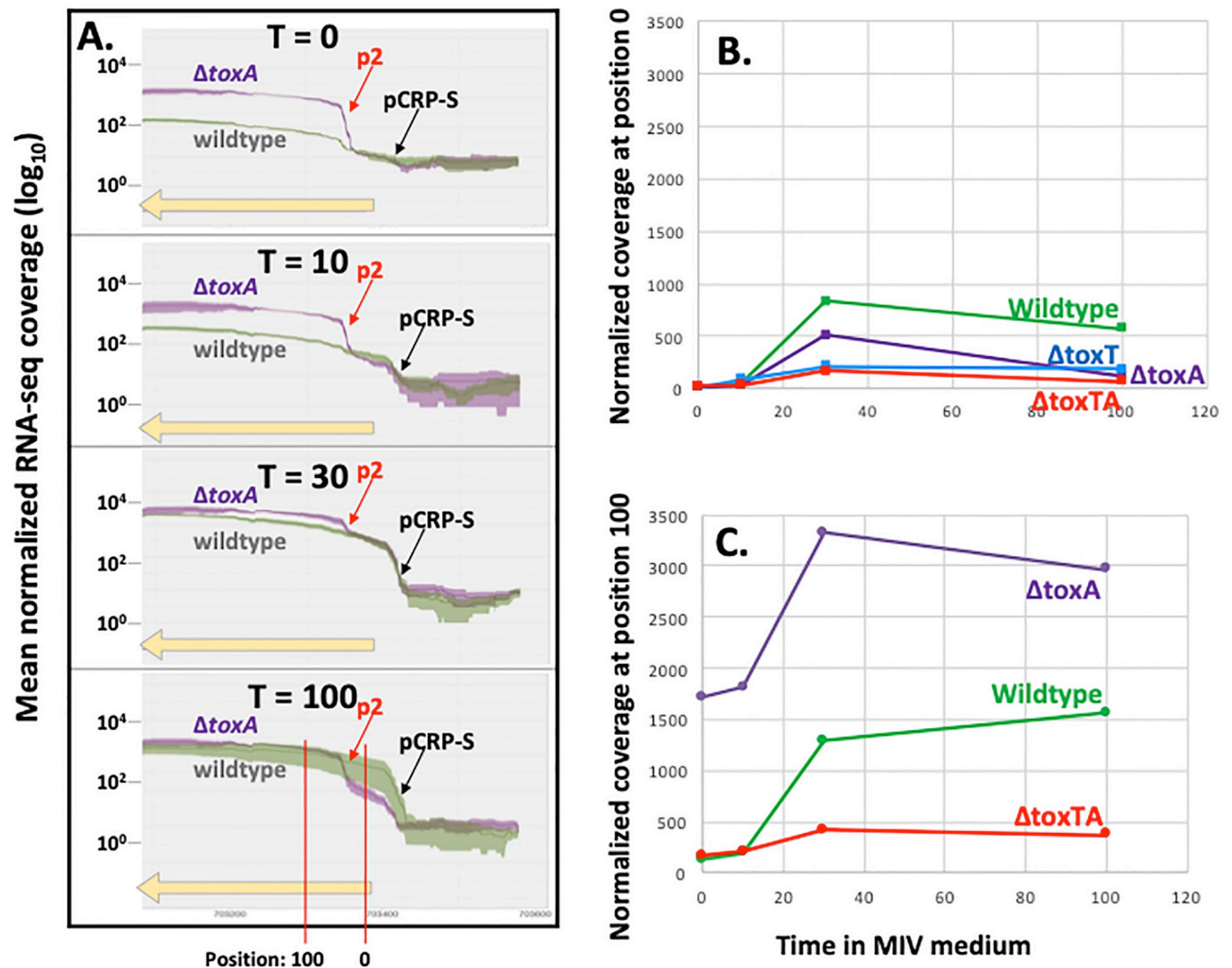


Fig 8. Sequencing read coverage of the *H. influenzae toxTA* promoter region. A. The green (KW20) and purple ($\Delta toxA$) lines indicate mean coverage normalized by library size using DESeq2 [size factors] at each position; shaded areas indicate standard errors. The yellow horizontal arrow indicates the 5' half of *toxT* (note that in this figure transcription is from right to left). B. and C. Time course of normalized read coverage at two specific positions in the *toxTA* operon. B. Position 0 = *toxA* start codon. C. Position 100.

<https://doi.org/10.1371/journal.pone.0217255.g008>

(transcription from P_{CRP-S}) was reduced by all of the *toxTA* deletions. This was unexpected, and suggests that this promoter may have unusual properties, since coverage of other CRP-S genes was not similarly affected. The *toxA* deletion caused the predicted increase in coverage at position 100 (Fig 8C), but the *toxTA* deletion unexpectedly reduced rather than increased coverage at this position ~3-fold from the wildtype level, even though this construct retains the first 150 bp of the operon, including P2. This reduction was not accounted for by the reduction in transcripts from P_{CRP-S} , suggesting that high-level transcription from the *toxTA* P2 promoter only occurs when ToxT is present and ToxA is absent. This could mean either that ToxT directly binds the P2 promoter to induce transcription, which seems unlikely given its lack of DNA-binding domain, or that the presence of ToxT disrupts binding of a secondary repressor of the operon, such as a noncognate antitoxin [25]. Alternatively, it is possible that the reduced transcript levels in the $\Delta toxTA$ mutant instead reflect reduced transcript stability in this mutant.

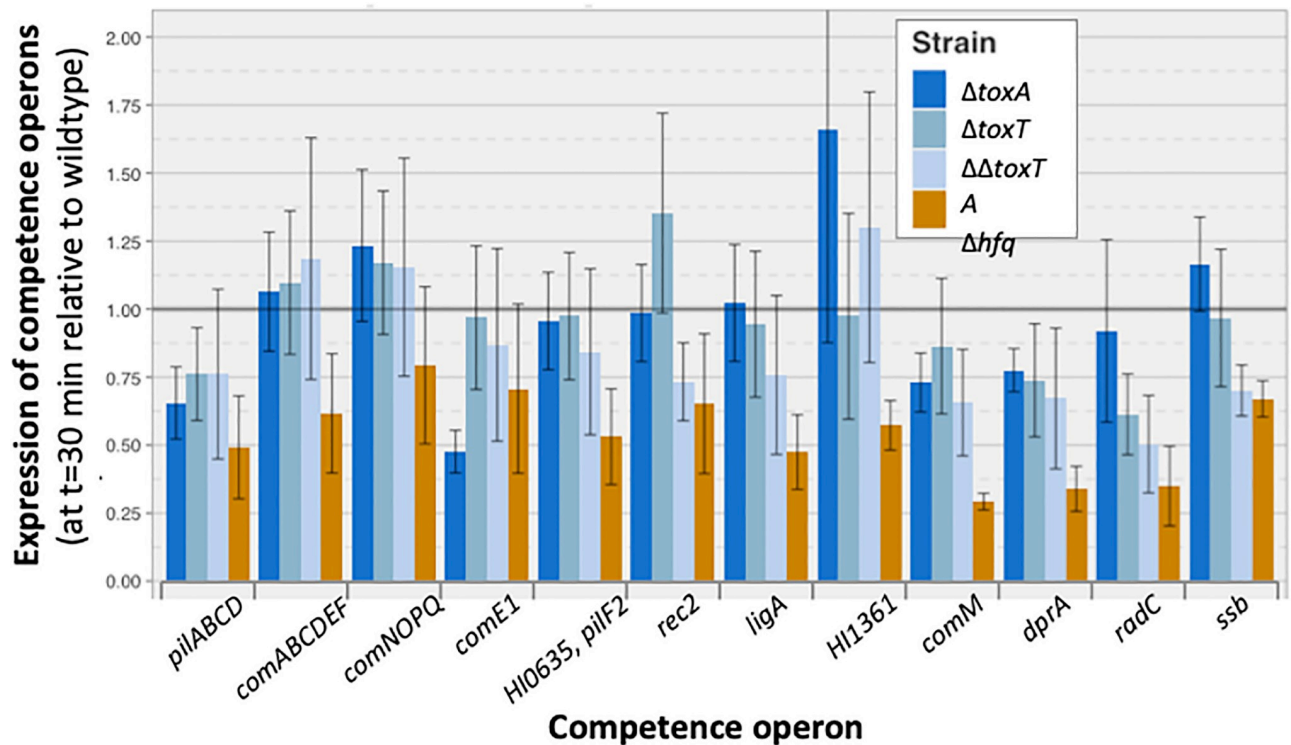


Fig 9. RNA-seq analysis of *H. influenzae* *toxTA* effects on competence-operon transcript levels. Bars show the relative transcript levels (as FPKM) of competence operons in four different mutants after 30 minutes of competence induction: $\Delta toxA$: dark blue, $\Delta toxT$: blue, $\Delta \Delta toxT$: light blue, Δhfq : brown. Transcript levels of each operon are relative to levels in wildtype cells at the same time point (grey horizontal bar). Error bars indicate standard errors of samples from three replicate cultures.

<https://doi.org/10.1371/journal.pone.0217255.g009>

Unopposed ToxT does not block induction of the competence regulon

Transcript levels of the competence operons that these regulators induce were also normal or near-normal in the $\Delta toxA$ mutant at 30 min after transfer to MIV, the time when competence-induced gene transcription is normally highest (Fig 9). Modest decreases were seen for some operons, but these are not expected to cause the absolute competence defect, for two reasons. First, competence gene transcript levels at this time were very similar between the $\Delta toxA$ mutant, which cannot take up any DNA or produce any transformants (dark blue bars), and the $\Delta toxT$ and $\Delta \Delta toxT$ mutants (other blue bars), which have normal competence. Second, an unrelated regulatory defect mutation, a knockout of *hfq*, causes a more extreme reduction in transcript levels at 30 min (brown bars) but this causes a much less extreme competence defect (only 10–20 fold rather than $>10^6$ -fold; green line in Figure B in S1 File). Mutation of *toxTA* genes also did not substantially change transcript levels of the *sxy*, *crp* and *cya* genes encoding the competence regulon regulators Sxy, CRP, and adenylate cyclase (Figure J in S1 File). At $t = 100$ the $\Delta toxA$ mutant showed a stronger reduction in RNA-seq coverage of competence genes (Figure K in S1 File), however this cannot explain the competence defect and its significance is unclear. The severe competence defect caused by unopposed *toxT* expression was also not explained by transcript level changes in other genes (Table E in S1 File).

Related toxins may suggest mechanism of action for ToxT

Since examination of gene expression shed little light on how the ToxT toxin prevents competence, and it has no close homologs with characterized functions, we considered the modes of

action of other Type II toxins. The most common type II toxins (e.g. RelE) act as translation-blocking ribonucleases, but several alternative modes of action are also known, and some newly discovered toxins lack identified activities [14]. The Pfam and TAFinder databases assign the *H. influenzae* ToxT protein to the ParE/RelE toxin superfamily, whose characterized members include both gyrase inhibitors and ribonucleases that arrest cell growth by cleaving mRNAs and other RNAs [2,12,13].

Unopposed toxin does not inhibit gyrase

If ToxT inhibited gyrase we would expect the RNA-seq data to show that transfer to MIV caused increased transcript levels of *gyrA* (HI1264) and *gyrB* (HI0567) and reduced levels of *topA* (HI1365), since these genes have opposing activities and compensatory regulation by DNA supercoiling [26]. However, these genes' coverage levels were similar in wildtype and all *toxTA* mutants, during both exponential growth and competence development. The SOS-response genes *lexA*, *recA*, *recN*, *recX*, *ruvA* and *impA* [27] were also not induced.

Unopposed toxin does not cleave competence-induced mRNAs at specific sites or sequences

The best-studied homologs of the *toxT* toxin act by cleaving mRNAs at positions near their 5' ends during their translation on the ribosome [28,29]. Because the resulting 'non-stop' mRNAs lack in-frame stop codons and cannot undergo the normal ribosome-release process, this causes a general block to translation [30] which is predicted to arrest cell growth until normal translation can be restored [31]. Thus we considered whether ToxT might prevent competence by one of two mechanisms. First, ToxT might specifically cleave the 5' ends of competence-gene transcripts, eliminating their function without significantly changing their overall RNA-seq coverage levels or otherwise interfering with essential cell functions. Visual inspection of RNA-seq coverage of all positions within the competence operons did not reveal any anomalies that might indicate that the mRNA in $\Delta toxA$ cells had been inactivated either by cleavage at specific sites or by random cleavage near the 5' end [32]. As an example, Figure L in S1 File compares read coverage across the *comNOPQ* operon in wildtype and $\Delta toxA$ cultures after 30 min in MIV.

Because mRNA sequences preferred by an RNA-cleaving toxin [33] are expected to be depleted from RNA-seq reads, we also used DE-kupl [34] to look for differences in kmer frequencies between RNA-seq samples from cells with and without active toxin. No significant differences were found.

To detect cleavage that was neither position-specific or sequence-specific, we examined the insert sizes of our RNA-seq sequencing libraries by comparing the spanning-length distributions of paired-end sequencing reads among strains. Because independent library preparations had different insert sizes, comparisons were limited to samples prepared at the same time. Fig 10 shows that the $\Delta toxA$ samples from library batch 1 had shorter fragment sizes than the KW20 samples from the same batch, and that the difference increased as the time after competence induction increased. This supports the hypothesis that the extreme lack of competence in $\Delta toxA$ cultures is due to non-specific ToxT cleavage of mRNAs. This mechanism is consistent with those of homologous HigB/RelE toxins, which inhibit translation by cleavage of mRNA at the ribosomal A-site [35,36].

Discussion

Our investigation into why a HI0659 knockout prevents competence has provided a simple answer: HI0659 encodes an antitoxin (ToxA) needed to block the expression and competence-

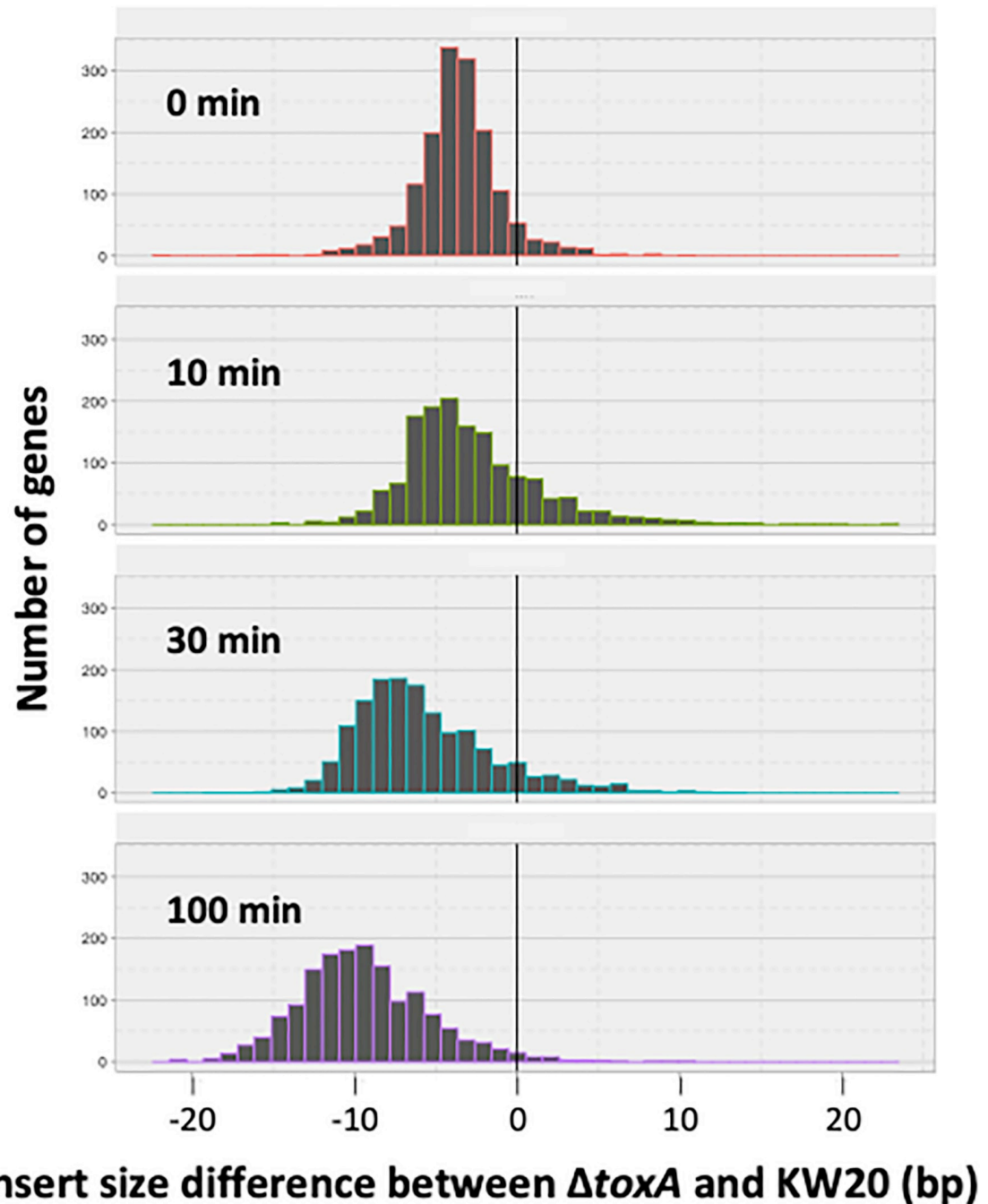


Fig 10. Distribution of insert-size differences between *H. influenzae* RNA-seq libraries prepared at the same time. Distribution of insert length differences between KW20 (kw20_A and kw20_B samples) and $\Delta toxA$ (antx_A samples) after 0, 10, 30 and 100 minutes in MIV.

<https://doi.org/10.1371/journal.pone.0217255.g010>

preventing activity of the toxin encoded by HI0660 (ToxT). But this answer has generated a number of new questions that we have only been able to partially answer. Why is competence controlled by a toxin/antitoxin system? How does it completely abolish DNA uptake and transformation without causing significant cell death? Do its effects in wildtype cells confer any benefit to the cells, either generally or specific to competence?

Several findings support the conclusion that HI0660 and HI0659 encode proteins that function as a toxin/antitoxin pair. First is the similarity of the encoded ToxT and ToxA proteins to biochemically characterized toxin and antitoxin proteins of the RelE/ParE families. Second, and the strongest evidence, is the restoration of normal DNA uptake and transformation to antitoxin-knockout cells when the putative toxin is also knocked out. Third is the regulatory similarity between this system and the *hicAB* system of *E. coli*.

How did the *toxTA* operon come to be in the *H. influenzae* genome and under competence regulation?

Phylogenetic analysis showed that *H. influenzae* acquired its *toxTA* operon by horizontal transfer, either into a deep ancestor of the Pasteurellaceae or more recently by independent transfers into ancestors of *H. influenzae* and *A. pleuropneumoniae*. The closest relatives of the *H. influenzae toxTA* genes are in the distantly related Firmicutes, with homologs especially common in *Streptococcus* species. Since the Streptococci and Pasteurellaceae share both natural competence and respiratory-tract niches in many mammals, there may have been frequent opportunities for horizontal transfer between them.

We do not know how the *toxTA* operon came to be under CRP-S regulation. The *toxTA* operon's strong regulatory parallels with the *E. coli hicAB* system suggest that toxin-antitoxin systems with similar regulation and function have adopted similar roles in separate instances, a phenomenon which is more likely in toxin antitoxin systems as they undergo frequent horizontal transfers and are often under strong selective pressure. The *sxy* gene and the CRP-S promoters it regulates are not known outside of the Gamma-Proteobacteria sub-clade that contains the Vibrionaceae, Enterobacteraceae, Pasteurellaceae and Orbaceae [11]. Thus, it would be interesting to examine the regulation and function of the *toxTA* homologs outside the Pasteurellaceae to determine when and where it adopted a regulatory role and the mechanism of the toxic activity. Examining these homologs could give insight into both the mechanism of action of the *H. influenzae toxTA* system, and its evolutionary history.

How does unopposed ToxT prevent DNA uptake and transformation?

The transformation defect caused by deletion of the antitoxin gene *toxA* is very severe, so it was surprising that RNA-seq analysis detected only few and minor changes in transcript levels of competence genes. Instead, the best explanation is that ToxT is an mRNA-cleaving ribonuclease, whose activity causes a general block to translation that prevents functioning of the induced competence genes. The most direct evidence is the decrease in insert size distributions seen in $\Delta toxA$ mutants, but this conclusion is also supported by the combination of regulatory similarities between the *toxTA* and *hicAB* systems and by sequence and predicted structural similarities between the ToxT protein and HigB ribonuclease toxins.

Why then does the $\Delta toxA$ mutant not suffer from growth arrest or toxicity?

Part of the explanation is that mRNAs encoding functional ToxT are only expressed after cells have been transferred to competence-inducing starvation medium, a condition that severely slows cell growth and division even in wildtype cells. Detecting the predicted competence-specific toxicity is further complicated by the uneven distribution of transformability in competence-induced cells. Co-transformation experiments using multiple unlinked markers consistently show that no more than half, and sometimes as little as 10%, of the cells in a MIV-treated culture produce recombinants [6]. We do not know whether only the transforming cells express the competence genes or all cells express them but some fail to correctly assemble the DNA uptake or recombination machinery. If only a modest fraction of the cells in a

competent culture are expressing the toxin then any toxic effect on culture growth and survival will be more difficult to detect.

Does this operon confer any benefit (or harm) on *H. influenzae*?

Why have a competence-regulating toxin/antitoxin system at all, when it has no detectable effect on competence unless its antitoxin component is defective? Although regulatory parallels with the *hicAB* system suggest that CRP-S regulation is not incidental, we found no direct evidence of any toxin-dependent alteration to the normal development of competence. Production of Sxy is subject to post-transcriptional regulation by the availability of nucleotide precursors [9,10], and we have elsewhere proposed that DNA uptake is an adaptation to obtain nucleotides when nucleotide scarcity threatens to arrest DNA replication forks [6]. In this context, competence-induction of the *toxTA* operon may be a specialization to help cells survive, by slowing or arresting protein synthesis until the nucleotide supply is restored.

On the other hand, the high frequency of deletions that remove either complete *toxTA* or both promoters (35%) indicates that the operon is dispensable. And the even higher frequency of toxin-inactivating deletions in the presence of intact antitoxin genes and CRP-S promoter (51%), coupled with the absence of any deletion that inactivates antitoxin but preserves toxin, indicates that unopposed toxin is indeed harmful under some natural circumstances. This may indicate that the toxin-antitoxin system represents merely a selfish genetic element which has become integrated into the *H. influenzae* genome and coincidentally fallen under CRP-S regulation [37]. This element may therefore be simply “junk DNA” which serves no function. Under this hypothesis, the mild purifying selection we see on the antitoxin gene would be lost in the *H. influenzae* strains with nonfunctional copies of the toxin gene. It is also possible that the *toxA* gene is beneficial even in the absence of its cognate toxin, which is under purifying selection even though most strains analyzed do not have a functional *toxT* counterpart. For example, the presence of a genomic antitoxin gene may counter the “plasmid addiction” effect of a plasmid bearing a similar toxin-antitoxin gene [37], perhaps limiting the risk of taking up foreign DNA. Unfortunately, the function of most toxin-antitoxin systems is poorly understood, and in this paper we are not yet able to conclusively determine the role and function of the *toxTA* system.

We have examined the *toxTA* operon from many angles and answered our initial question of why *toxA* knockout prevents competence in *H. influenzae*, but have raised new questions whose eventual answers we hope will give us greater insight not just into the *toxTA* system, but competence regulation in general. A number of desirable follow-up experiments could improve understanding of the *toxTA* system, particularly complementation experiments to determine whether ToxA expression in $\Delta toxA$ can restore competence, and whether ToxT expression in $\Delta toxTA$ can block competence. In future work, it would also be valuable to express ToxT and ToxA in *E. coli* on separate plasmids to examine the system’s toxicity and effect on competence.

Methods

Bacterial strains, plasmids, and growth conditions

Bacterial strains used in this work are listed in Table A of [S1 File](#). *Escherichia coli* strain DH5 α [F80*lacZ* #(*lacIZYA-argF*) endA1] was used for all cloning steps; it was cultured in Luria-Bertani (LB) medium at 37°C and was made competent with rubidium chloride according to the method provided in the QIAexpressionist manual protocol 2 (Qiagen). When antibiotic selection was required, 100 μ g/mL ampicillin and 50 μ g/mL spectinomycin were used.

Haemophilus influenzae cells were grown in sBHI medium (Brain Heart Infusion medium supplemented with 10mg/mL hemin and 2mg/mL NAD) at 37°C in a shaking water bath (liquid cultures) or incubator (plates). *H. influenzae* strain Rd KW20 [38], the standard laboratory strain, was used as the wild type for all experiments. Mutant strains used in this study were marked deletion mutants in which the coding region of the gene was replaced by a spectinomycin resistance cassette, as well as unmarked deletion mutants derived from these strains; the generation of these mutant strains is described in [8]. Specifically, we used an unmarked deletion of HI0659 (HI0659-), marked and unmarked deletions of HI0660 (HI0660::spec, HI0660-), and a marked deletion of the whole operon (HI0659/HI0660::spec). Knockout mutants of *crp* and *sxy* have been described previously [20,39].

Actinobacillus pleuropneumoniae cells were grown in BHI-N medium (Brain Heart Infusion medium supplemented with 100µg/mL NAD) at 37°C. *A. pleuropneumoniae* strain HS143 [40] was used as the wild type for all experiments. Marked deletion mutants in which the gene of interest was replaced by a spectinomycin resistance cassette strains were generated for this study as described below. The HS143 genome region containing the homologs of the *Actinobacillus pleuropneumoniae* serovar 5b strain L20 APL_1357 and APL_1358 genes, plus approximately 1 kb of flanking sequence on each side, was PCR-amplified, ligated into Promega pGEM-T Easy and transformed into *E. coli*. Plasmid regions containing APL_1357, APL_1358, or both genes were deleted from the pGEM-based plasmid by inverse PCR, and the amplified fragments were blunt-end ligated to the spectinomycin resistance cassette [41] from genomic DNA of a *H. influenzae* *comN::spec* strain [8]. Plasmids linearized with *ScaI* were transformed into competent *A. pleuropneumoniae* HS143 and transformants were selected for spectinomycin resistance using 100µg/mL spectinomycin after 80 minutes of growth in nonselective medium.

Generation of competent stocks

To induce competence, *H. influenzae* and *A. pleuropneumoniae* were cultured in sBHI or BHI-N respectively and transferred to the competence-inducing starvation medium MIV [42] when they reached an optical density at 600nm (OD₆₀₀) of approximately 0.25 [43]. After incubation with gentle shaking at 37°C for a further 100 min (*H. influenzae*) or 150 min (*A. pleuropneumoniae*), cells were transformed or frozen in 16% glycerol at -80 °C for later use.

Transformation assays

Transformation of MIV-competent cells. Transformation assays were carried out as described by Poje and Redfield [43]. MIV-competent *H. influenzae* or *A. pleuropneumoniae* cells were incubated at 37°C for 15 minutes with 1µg/ml DNA, then DNaseI (10µg/mL) was added and cultures were incubated for 5 minutes to ensure no DNA remained in the medium. *H. influenzae* cultures were transformed with MAP7 genomic DNA [44], which carries resistance genes for multiple antibiotics, while *A. pleuropneumoniae* cultures were transformed with genomic DNA from an *A. pleuropneumoniae* strain with spontaneous nalidixic acid resistance (generated in this lab). Cultures were diluted and plated on both plain and antibiotic-containing plates (2.5µg/mL novobiocin for *H. influenzae* cultures, 20µg/mL nalidixic acid for *A. pleuropneumoniae* cultures) and transformation frequencies were calculated as the ratio of transformed (antibiotic-resistant) cells to total cells. For *A. pleuropneumoniae*, transformed cells were given 80 minutes of expression time in BHI-N before plating.

Time courses in rich medium. *H. influenzae* cells from frozen stocks of overnight cultures were diluted in fresh sBHI and incubated with shaking at 37°C. Periodically, the OD₆₀₀

was measured, and at predetermined optical densities aliquots of the culture were removed and transformed with MAP7 DNA and plated as described above.

Bioscreen growth analysis. The Bioscreen C apparatus (BioScreen Instruments Pvt. Ltd.) was used to measure growth. Cells frozen from overnight cultures were pre-grown at low density in sBHI, and 300 μ L aliquots of 100-fold dilutions were placed into 20 replicate wells of a 100-well Bioscreen plate. Wells at the edges of the plate were filled with medium alone as controls. Cells were grown in the Bioscreen at 37°C for 18 hours with gentle shaking, and OD₆₀₀ readings were taken every 10 minutes. Readings were corrected by subtracting the OD₆₀₀ measured for medium-only controls, and replicates for each strain were averaged at each time point to generate growth curves. Doubling times were calculated for each strain from the subset of time points that represents exponential growth phase, as determined by linearity on a semi-log plot of time versus OD₆₀₀.

Competence growth and survival time course. Cells were grown in sBHI to a density of $\sim 2 \times 10^8$ cfu/ml (OD₆₀₀ = 0.075) and transferred to MIV. After 100 min (time for maximum competence development, an aliquot of each culture was diluted 1/10 into fresh sBHI for recovery and return to normal growth. A fraction of each culture was incubated in a shaking water bath, and aliquots of the initial and 'recovery' sBHI cultures were also grown and monitored in a Bioscreen incubator.

Cyclic AMP competence induction. *H. influenzae* cells in sBHI were incubated with shaking to an OD₆₀₀ of approximately 0.05. Cultures were split and 1mM cAMP was added to one half. At an OD₆₀₀ of approximately 0.3, aliquots were transformed with MAP7 DNA and plated as described above.

Phylogenetic analysis. A nucleotide BLAST search (discontinuous MEGABLAST) and a protein BLAST search against translated nucleotide databases (tBLASTn) were used to identify homologs of the HI0659 and HI0660 genes [45]. Protein sequences found by the tBLASTn search were retained for analysis if they showed greater than 60% coverage and greater than 40% identity to the *H. influenzae* query sequence. For species with matching sequences in multiple strains, the sequence from only one strain was kept.

For species in which homologs of HI0659 and HI0660 were found next to one another, amino acid sequences of concatenated matrices were aligned by multiple-sequence alignment using MAFFT, version 7.220 [46], run from modules within Mesquite version 3.02 [47]. The L-INS-I alignment method was used due to its superior accuracy for small numbers of sequences. After inspection of the alignments, poorly-aligning sequences were removed from the analysis, and alignment was repeated.

Phylogenetic trees were generated using the RAxML [48] maximum likelihood tree inference program, run via the Zephyr package of Mesquite. For each gene, 50 search replicates were conducted, using the PROTGAMMAAUTO option to allow RAxML to automatically select the best protein evolution model to fit the data. Since these trees were found to correspond exactly to a set of trees generated using the PROTGAMMAJTT model, this faster model was used to generate a majority-rules consensus tree from 1000 bootstrap replicates for each gene.

Analysis of natural deletions. 181 publicly available *H. influenzae* genomes were downloaded from NCBI and the Sanger centre. Genomes were re-annotated using Prokka v1.11 [49], and the pangenome was calculated using Roary v3.5.1 [50] with a minimum blastp threshold of 75. The *toxA* gene cluster in the pangenome was identified by finding the gene cluster that contained the *toxA* gene from Rd KW20, and the *hicA* cluster was identified by finding the gene cluster that contained the *hicA* gene from PittAA. 2300 bp genome sequences centered on *toxA* and/or *hicA* were extracted from all *H. influenzae* genomes containing recognizable *toxA* and/or *hicB* genes, and aligned by MAFFT. For strains that lacked recognizable *toxA* or *hicB*, sequences adjacent to the genes that normally flanked each operon were

extracted. K_a/K_s and pairwise distance were calculated for each gene using SeqinR v 3.4–5 [51] with codon aware gene alignments were made using Prank (v.100802).

RNA-seq analysis

Sample preparation. Cell cultures of *H. influenzae* strain Rd, Δcrp and Δsxy derivatives, and $\Delta toxTA$ mutants were grown in sBHI to an OD_{600} of 0.2–0.25, then transferred to MIV. Aliquots of cells were removed just prior to transfer to MIV, and after 10, 30, and 100 minutes in MIV, and immediately mixed with Qiagen RNeasy Protect (#76526) to stabilize RNA. Cells were pelleted and frozen, and RNA was later extracted from thawed pellets using the Qiagen RNeasy Min-elute Cleanup Kit (#74204). Contaminating DNA was removed with Ambion Turbo DNase (#AM2238), and ribosomal RNA was depleted using the Illumina Ribo-Zero rRNA Removal kit (#MRZMB126). Sequencing libraries were prepared using TruSeq mRNA v2 library preparation kit, according to manufacturer's instructions (Illumina). Libraries were pooled and sequenced on a HiSeq 2500, generating paired-end 100 bp reads.

Data analysis pipeline. FASTQ files were analysed using the FASTQC tool (Andrews, 2015) to confirm read quality. Reads were aligned to the *H. influenzae* Rd KW20 reference genome sequence using the Burrows-Wheeler Alignment tool (BWA) algorithm `bwa mem` [52]. Differential coverage analysis was performed using the DESeq2 package, v.1.6.3 [53]. Specifically, the function `DESeqDataSetFromMatrix()` was used to generate a dataset to compare reads from each mutant strain reads from the wild-type control based on their strain, sample time point, and the interaction between the two parameters. The function `DESeq()` was called to determine which genes were differentially expressed based on these parameters, using p-values adjusted for a B-H false-discovery rate [54] of 0.1 as a cut-off to determine significance, after normalizing total read counts and variances.

Supporting information

S1 File. All supporting materials. RNAseq analysis methods, Tables A-E, and Figures A-L. (DOCX)

Acknowledgments

We thank Lauri Lintott for helpful discussions, Charles Thompson for the use of the BioScreen Analyzer, and Anni Zhang and Yvonne Yiu for technical assistance. Sequencing work was performed at the Sequencing and Bioinformatics Consortium at the University of British Columbia.

Author Contributions

Conceptualization: Hailey Findlay Black, Joshua Chang Mell, Rosemary J. Redfield.

Data curation: Hailey Findlay Black, Scott Mastromatteo, Rachel L. Ehrlich, Corey Nislow, Joshua Chang Mell.

Funding acquisition: Corey Nislow, Joshua Chang Mell, Rosemary J. Redfield.

Investigation: Hailey Findlay Black, Sunita Sinha, Joshua Chang Mell.

Methodology: Hailey Findlay Black, Scott Mastromatteo, Sunita Sinha, Joshua Chang Mell.

Project administration: Corey Nislow, Rosemary J. Redfield.

Software: Scott Mastromatteo.

Supervision: Rosemary J. Redfield.

Visualization: Scott Mastromatteo, Rosemary J. Redfield.

Writing – original draft: Hailey Findlay Black.

Writing – review & editing: Hailey Findlay Black, Scott Mastromatteo, Sunita Sinha, Corey Nislow, Joshua Chang Mell, Rosemary J. Redfield.

References

1. Harms A, Brodersen DE, Mitarai N, Gerdes K. Toxins, targets, and triggers: an overview of toxin-antitoxin biology. *Molecular cell*. 2018; 70(5):768–84. <https://doi.org/10.1016/j.molcel.2018.01.003> PMID: 29398446
2. Chan WT, Espinosa M, Yeo CC. Keeping the wolves at bay: antitoxins of prokaryotic type II toxin-antitoxin systems. *Frontiers in Molecular Biosciences*. 2016; 3:9. <https://doi.org/10.3389/fmolb.2016.00009> PMID: 27047942
3. Hall AM, Gollan B, Helaine S. Toxin-antitoxin systems: reversible toxicity. *Current Opinion in Microbiology*. 2017; 36:102–10. <https://doi.org/10.1016/j.mib.2017.02.003> PMID: 28279904
4. Ambur OH, Engelstädter J, Johnsen PJ, Miller EL, Rozen DE. Steady at the wheel: conservative sex and the benefits of bacterial transformation. *Philos T R Soc B*. 2016; 371(1706): <https://doi.org/10.1098/rstb.2015.0528> PMID: 27619692
5. Johnston C, Martin B, Fichant G, Polard P, Claverys J-P. Bacterial transformation: distribution, shared mechanisms and divergent control. *Nat Rev Microbiol*. 2014; 12: 181–196. <https://doi.org/10.1038/nrmicro3199> PMID: 24509783
6. Mell JC, Redfield RJ. Natural competence and the evolution of DNA uptake specificity. *J Bacteriol*. 2014; 196(8):1471–1483. <https://doi.org/10.1128/JB.01293-13> PMID: 24488316
7. Redfield RJ, Cameron ADS, Qian Q, Hinds J, Ali TR, Kroll JS, et al. A novel CRP-dependent regulon controls expression of competence genes in *Haemophilus influenzae*. *J Mol Biol*. 2005; 4(8):735–747.
8. Sinha S, Mell JC, Redfield RJ. Seventeen Sxy-dependent cyclic AMP receptor protein site-regulated genes are needed for natural transformation in *Haemophilus influenzae*. *J Bacteriol*. 2012; 194(19):5245–5254. <https://doi.org/10.1128/JB.00671-12> PMID: 22821979
9. Macfadyen LP, Chen D, Vo HC, Liao D, Sinotte R, Redfield RJ. Competence development by *Haemophilus influenzae* is regulated by the availability of nucleic acid precursors. *Mol Microbiol*. 2001; 40(3):700–707. <https://doi.org/10.1046/j.1365-2958.2001.02419.x> PMID: 11359575
10. Sinha S, Mell JC, Redfield R. The availability of purine nucleotides regulates natural competence by controlling translation of the competence activator Sxy. *Mol Microbiol*. 2013; 88(6):1106–1119. <https://doi.org/10.1111/mmi.12245> PMID: 23663205
11. Cameron ADS, Redfield RJ. Non-canonical CRP sites control competence regulons in *Escherichia coli* and many other gamma-proteobacteria. *Nucleic Acids Res*. 2006; 34(20): 6001–6014. <https://doi.org/10.1093/nar/gkl734> PMID: 17068078
12. Jorgensen MG, Pandey DP, Jaskolska M, Gerdes J. HicA of *Escherichia coli* defines a novel family of translation-independent mRNA interferases in bacteria and archaea. *J Bacteriol*. 2009; 191(4):1191–1199. <https://doi.org/10.1128/JB.01013-08> PMID: 19060138
13. Christensen-Dalsgaard M, Gerdes K. Two *higBA* loci in the *Vibrio cholerae* superintegron encode mRNA cleaving enzymes and can stabilize plasmids. *Mol Microbiol*. 2006; 62:397–411. <https://doi.org/10.1111/j.1365-2958.2006.05385.x> PMID: 17020579
14. Makarova KS, Wolf YI, Koonin EV. Comprehensive comparative-genomic analysis of Type 2 toxin-antitoxin systems and related mobile stress elements in prokaryotes. *Biology Direct*. 2009; 4(19): <https://doi.org/10.1186/1745-6150-4-19> PMID: 19493340
15. Kelley LA, Mezulis S, Yates CM, Wass MN, Sternberg MJ. The Phyre2 web portal for protein modeling, prediction and analysis. *Nature Protocols*. 2015; 10(6):845. <https://doi.org/10.1038/nprot.2015.053> PMID: 25950237
16. Letunic I. Interactive Tree Of Life (iTOL): an online tool for phylogenetic tree display and annotation. *Bioinformatics*. 2007; 23(1):127–128. <https://doi.org/10.1093/bioinformatics/btl529> PMID: 17050570
17. Maughan H, Redfield RJ. Extensive variation in natural competence in *Haemophilus influenzae*. *Evolution*. 2009; 63(7):1852–1866. <https://doi.org/10.1111/j.1558-5646.2009.00658.x> PMID: 19239488

18. Dorocicz IR, Williams PM, Redfield RJ. The *Haemophilus influenzae* adenylate cyclase gene: cloning, sequence, and essential role in competence. *J Bacteriol.* 1993; 175(22):7142–7149. <https://doi.org/10.1128/jb.175.22.7142-7149.1993> PMID: 8226661
19. Page R, Peti W. Toxin-antitoxin systems in bacterial growth arrest and persistence. *Nature Chemical Biology.* 2016; 12:208–214. <https://doi.org/10.1038/nchembio.2044> PMID: 26991085
20. Williams PM, Bannister LA, Redfield RJ. The *Haemophilus influenzae* sxy-1 mutation is in a newly identified gene essential for competence. *J Bacteriol.* 1994; 176(22):6789–6794. <https://doi.org/10.1128/jb.176.22.6789-6794.1994> PMID: 7961436
21. Ma C, Redfield RJ. Point Mutations in a Peptidoglycan Biosynthesis Gene Cause Competence Induction in *Haemophilus influenzae*. *J Bacteriol.* 2000; 182(12):3323–3330. <https://doi.org/10.1128/jb.182.12.3323-3330.2000> PMID: 10852860
22. Overgaard M, Borch J, Jorgensen MG, Gerdes K. Messenger RNA interferase *RelE* controls *relBE* transcription by conditional cooperativity. *Mol Microbiol.* 2008; 69(4):841–857. <https://doi.org/10.1111/j.1365-2958.2008.06313.x> PMID: 18532983
23. Turnbull KJ, Gerdes K. HicA toxin of *Escherichia coli* derepresses *hicAB* transcription to selectively produce HicB antitoxin. *Mol Microbiol.* 2017; 104(5): 781–792. <https://doi.org/10.1111/mmi.13662> PMID: 28266056
24. Sinha S, Cameron ADS, Redfield RJ. Sxy induces a CRP-S regulon in *Escherichia coli*. *J Bacteriol.* 2009; 191(16):5180–5195. <https://doi.org/10.1128/JB.00476-09> PMID: 19502395
25. Goeders N, Van Melder L. Toxin-antitoxin systems as multilevel interaction systems. *Toxins.* 2014; 6(1):304–324. <https://doi.org/10.3390/toxins6010304> PMID: 24434905
26. Gmuender H, Kuratli K, Di Padova K, Gray CP, Keck W, Evers S. Gene expression changes triggered by exposure of *Haemophilus influenzae* to novobiocin or ciprofloxacin: combined transcription and translation analysis. *Genome Res.* 2001; 11: 28–42. PMID: 11156613
27. Sweetman WA, Moxon ER, Bayliss CD. Induction of the SOS regulon of *Haemophilus influenzae* does not affect phase variation rates at tetranucleotide or dinucleotide repeats. *Microbiology.* 2005; 151(8):2751–63.
28. Hurley JM, Cruz JW, Ouyang M, Woychik NA. Bacterial toxin RelE mediates frequent codon-independent mRNA cleavage from the 5' end of coding regions in vivo. *J Biol Chem.* 2011; 286:14770–14778. <https://doi.org/10.1074/jbc.M110.108969> PMID: 21324908
29. Goeders N, Dreze P-L, Van Melder L. Relaxed cleavage specificity within the RelE toxin family. *J Bacteriol.* 2013; 195(11): 2541–2549. <https://doi.org/10.1128/JB.02266-12> PMID: 23543711
30. Tollervey D. Molecular Biology: RNA lost in translation. *Nature.* 2006; 440: 425–426. PMID: 16554791
31. Pandey DP, Gerdes K. Toxin-antitoxin loci are highly abundant in free-living but lost from host-associated prokaryotes. *Nucleic Acids Res.* 2005; 33(3):966–976. <https://doi.org/10.1093/nar/gki201> PMID: 15718296
32. Gordon GC, Cameron JC, Pflieger BF. RNA sequencing identifies new RNase III cleavage sites in *Escherichia coli* and reveals increased regulation of mRNA. *mBio.* 2017; 8(2):e00128–17. <https://doi.org/10.1128/mBio.00128-17> PMID: 28351917
33. Masuda H, Inouye M. Toxins of prokaryotic toxin-antitoxin systems with sequence-specific endoribonuclease activity. *Toxins.* 2017; 9(4):140.
34. Audoux J, Philippe N, Chikhi R, Salson M, Gallopin M, Gabriel M, et al. DE-kupl: exhaustive capture of biological variation in RNA-seq data through k-mer decomposition. *Genome Biology.* 2017; 18(1):243. <https://doi.org/10.1186/s13059-017-1372-2> PMID: 29284518
35. Pedersen K, Zavialov AV, Pavlov MY, Elf J, Gerdes K, Ehrenberg M. The Bacterial Toxin RelE Displays Codon-Specific Cleavage of mRNAs in the Ribosomal A Site. *Cell.* 2003; 112(1):133–140.
36. Neubauer C, Gao Y-G, Andersen KR, Dunham CM, Kelley AC, Hentschel J, et al. The Structural Basis for mRNA Recognition and Cleavage by the Ribosome-Dependent Endonuclease RelE. *Cell.* 2009; 139(6):1084–1095. <https://doi.org/10.1016/j.cell.2009.11.015> PMID: 20005802
37. Ramisetty BC, Santhosh RS. Endoribonuclease type II toxin-antitoxin systems: functional or selfish?. *Microbiology.* 2017; 163(7):931–9. <https://doi.org/10.1099/mic.0.000487> PMID: 28691660
38. Alexander HE, and Leidy G. Determination of inherited traits of *H. influenzae* by desoxyribonucleic acid fractions isolated from type-specific cells. *J Exp Med.* 1951; 93:345–359. <https://doi.org/10.1084/jem.93.4.345> PMID: 14824407
39. Chandler MS. The gene encoding cAMP receptor protein is required for competence development in *Haemophilus influenzae* Rd. *P Natl Acad Sci USA.* 1992; 89(5):1626–30.

40. Blackall PJ, Klaasen HL, van den Bosch H, Kuhnert P, Frey J. Proposal of a new serovar of *Actinobacillus pleuropneumoniae*: serovar 15. *Vet Microbiol*. 2002; 84(1–2):47–52. [https://doi.org/10.1016/s0378-1135\(01\)00428-x](https://doi.org/10.1016/s0378-1135(01)00428-x) PMID: 11731158
41. Tracy E, Ye F, Baker BD, Munson RS. Construction of non-polar mutants in *Haemophilus influenzae* using FLP recombinase technology. *BMC Mol Biol*. 2008; 9: <https://doi.org/10.1186/1471-2180-11-208>
42. Herriott RM, Meyer EY, Vogt M, Modan M. Defined medium for growth of *Haemophilus influenzae*. *J Bacteriol*. 1970; 101(2):513–6. PMID: 5308770
43. Poje G, Redfield RJ. Transformation of *Haemophilus influenzae*. *Methods Mol Med*. 2003; 71:57–70. <https://doi.org/10.1385/1-59259-321-6:57> PMID: 12374031
44. Barcak GJ, Chandler MS, Redfield RJ, Tomb JF. Genetic systems in *Haemophilus influenzae*. *Method Enzymol*. 1991 204:321–342.
45. Altschul SF, Gish W, Miller W, Myers EW, Lipman DJ. Basic Local Alignment Search Tool. *J Mol Biol*. 1990; 215(3):403–410. [https://doi.org/10.1016/S0022-2836\(05\)80360-2](https://doi.org/10.1016/S0022-2836(05)80360-2) PMID: 2231712
46. Katoh S. MAFFT multiple sequence alignment software version 7: improvements in performance and usability. *Mol Biol Evol*. 2013; 30:772–780. <https://doi.org/10.1093/molbev/mst010> PMID: 23329690
47. Maddison WP, Maddison DR. Mesquite: a modular system for evolutionary analysis. Version 3.02. 2013; <http://mesquiteproject.org>
48. Stamatakis A. RAxML Version 8: A tool for phylogenetic analysis and post-analysis of large phylogenies. *Bioinformatics*. 2014; 30(9):1312–1313. <https://doi.org/10.1093/bioinformatics/btu033> PMID: 24451623
49. Seemann T. Prokka: rapid prokaryotic genome annotation. *Bioinformatics*. 2014; 30(14):2068–2069. <https://doi.org/10.1093/bioinformatics/btu153> PMID: 24642063
50. Page AJ, Cummins CA, Hunt M, Wong VK, Reuter S, Holden MTG, et al. Roary: rapid large-scale prokaryote pan genome analysis. *Bioinformatics*. 2015; 31(22):3691–3693. <https://doi.org/10.1093/bioinformatics/btv421> PMID: 26198102
51. Charif D, Lobry JR. SeqinR 1.0–2: A contributed package to the R Project for statistical computing devoted to biological sequences retrieval and analysis. *Structural Approaches to Sequence Evolution*. Springer, Berlin, Heidelberg. 2007; https://doi.org/10.1007/978-3-540-35306-5_10
52. Li H, and Durbin R. Fast and accurate short read alignment with Burrows–Wheeler transform. *Bioinformatics*. 2009; 5(14):1754–1760.
53. Love M, Anders S, Huber W. Differential analysis of RNA-Seq data at the gene level using the DESeq2 package. Heidelberg: European Molecular Biology Laboratory (EMBL). 2013.
54. Benjamini Y, and Hochberg Y. Controlling the false discovery rate: a practical and powerful approach to multiple testing. *J R Stat Soc*. 1995; 57(1):285–300.